J Exp Biol Advance Online Articles. First posted online on 4 September 2014 as doi:10.1242/jeb.109991
Access the most recent version at http://jeb.biologists.org/lookup/doi/10.1242/jeb.109991

Do all frogs swim alike? The effect of ecological specialization on swimming kinematics in frogs.

Pavla Robovska-Havelkova[1], Peter Aerts[2,3], Zbynek Rocek[4], Tomas Prikryl[4], Anne-Claire Fabre[5] and Anthony Herrel[6,7]

1. Department of Zoology, Faculty of Science, University of South Bohemia, Çeské Budejovice, Czech Republic.

2. Department of Biology, University of Antwerp, Universiteitsplein 1, B-2610 Antwerpen, Belgium.

3. Department of Movement and Sports Sciences, University of Ghent, Watersportlaan 2, B-9000 Ghent, Belgium.

4. Department of Paleobiology, Geological Institute, Academy of Sciences, Prague, Czech Republic.

5. Evolutionary Anthropology, Duke University, Durham, North Carolina, 27708-0383, USA.

6. UMR 7179 C.N.R.S/M.N.H.N., Département d'Ecologie et de Gestion de la Biodiversité, 57 rue Cuvier, Case postale 55, 75231, Paris Cedex 5, France.

7. Ghent University, Evolutionary Morphology of Vertebrates, K.L. Ledeganckstraat 35, B-9000 Gent, Belgium.

Running title: frog swimming kinematics

pages: 17

tables: 4

figures: 6; supplementary figures: 6

Address for correspondence:

Anthony Herrel

UMR 7179 C.N.R.S/M.N.H.N.

Département d'Ecologie et Gestion de la Biodiversité

57 rue Cuvier, Case postale 55 — phone++33-140798120

75231 Paris Cedex 5 — fax : ++33-140793773

France — e-mail : anthony.herrel@mnhn.fr

Abstract

Frog locomotion has attracted wide scientific interest due to the unusual and derived morphology of the frog pelvic girdle and hind limb. Previous authors have suggested that the design of the frog locomotor system evolved towards a specialized jumping morphology early-on in the radiation of the group. However, data on locomotion in frogs are biased towards a few groups and most of the ecological and functional diversity remains unexplored. Here we examine the kinematics of swimming in eight species of frog with different ecologies. We use cineradiography to quantify movements of skeletal elements from the entire appendicular skeleton. Our results show that species with different ecologies do differ in the kinematics of swimming with the speed of limb extension and especially the kinematics of the mid-foot being different. Our results moreover suggest that this is not a phylogenetic effect as species from different clades with similar ecologies converge on the same swimming kinematics. These results suggest that it is important to analyze frog locomotion in a broader ecological and evolutionary context if one is to understand the evolutionary origins of this behavior.

Introduction

Frog locomotion has attracted wide scientific interest because of the unusual and highly derived morphology of these animals (Barclay, 1946; Estes and Reig, 1973; Zug, 1978; Frost et al., 2006). Frogs are characterized by a shortened trunk and tail, elongated ilia, and elongated hind limbs. This morphology has been interpreted as being associated with a jumping life style and thus it has been suggested that jumping evolved early-on in the evolution of the lineage (Gans and Parsons, 1966; Shubin and Jenkins, 1995; Jenkins and Shubin, 1998) and many recent studies have attempted to infer locomotion in basal frogs (Prikryl et al., 2009; Essner et al., 2010; Reilly and Jorgenses, 2011; Sigurdsen et al., 2012; Venczel and Szentesi, 2012; Jorgensen and Reilly, 2013). However, kinematic and electromyographic studies indicate strong similarities between the mechanics of swimming and jumping in some frogs (Emerson and De Jongh, 1980; Peters et al., 1996; but see Nauwelaerts and Aerts, 2003), implying that morphological features associated with these two locomotor modes may not be that different. This may, in turn, complicate inferences of locomotor modes from anatomy as is often done for extinct animals. Despite their rather uniform morphology, frogs are an ecologically diverse and speciose group with over 5000 known species (Frost et al., 2006). Moreover, animals with different ecologies have evolved different morphologies and show similar levels of locomotor performance (Moen et al., 2013) suggesting that locomotion may differ in animals with different ecologies.

To date most of our knowledge on frog locomotion is based on data for a limited set of derived frogs including ranoids (mostly ranids and bufonids; Calow and Alexander, 1973; Lutz and Rome, 1994; Kamel et al., 1996; Peters et al., 1996; Olson and Marsh, 1998; Gillis and Biewener, 2000; Nauwelaerts and Aerts, 2002, 2003, 2006; Nauwelaerts et al., 2001, 2004, 2005a,b; Johansson and Lauder, 2004; Stamhuis and Nauwelaerts, 2005) and highly specialized aquatic pipids (Gal and Blake, 1988; Richards and Biewener, 2007; Richards, 2008; Clemente and Richards, 2013). A comparison of swimming kinematics between the highly specialized aquatic pipids and more generalized terrestrial species showed differences in joint kinematics indicating differences in the underlying propulsive strategies of swimming across species (Richards, 2010). Although these data suggest that frogs with different ecologies differ in their limb kinematics, this remains to be tested using a broader sample of species with different ecologies and from different phylogenetic backgrounds. For example, the only study on swimming in primitive leiopelmatid frogs demonstrated an alternative swimming pattern consisting of an asymmetric swimming gait (Abourachid and Green, 1999) that may be related to the low locomotor speeds observed in these animals (Nauwelaerts and Aerts, 2002).

Here we explore the diversity in hind limb kinematics during the propulsive phase of swimming in frogs by studying 8 species of frogs from different families and with different ecologies (Table 1; Fig. 1). We include both species with different ecologies (aquatic, terrestrial and semi-aquatic) and different phylogenetic affinities. Given the importance of pelvic girdle movements during locomotion in frogs (Emerson, 1976; 1979; Videler and Jorna, 1985) we decided to use cineradiography rather than typical external high-speed video recordings to quantify swimming kinematics. Specifically, we test the hypothesis that species with different ecologies will differ in the kinematics of limb movement during swimming, with aquatic species showing greater velocities of movement and greater angular displacements at the distal-most joints associated with the rotation-powered swimming style observed in highly specialized swimmers (Richards, 2010).

Results

Descriptive kinematics

Swimming in all species involved limb extension with significant movements at the hip, knee, and ankle (Figs. 3-5; Supplementary figures 1-6). Whereas terrestrial and semi-aquatic species showed a clear proximo-distal extension sequence starting at the hip and ending at the ankle, this was not the case in specialized aquatic species where extension was initiated at the level of the knee, followed by the hip and the ankle. However, the greatest differences were observed in the movements at the distal-most segments (i.e. mid-foot angles). Whereas in all species movements at the proximal foot were observed resulting in an extension of the foot fairly late in the kick, in specialized aquatics, the distal-most part of the foot (mid-foot 2) was extended throughout the extension cycle. In the other species this angle showed little change and the distal foot remained extended throughout the extension cycle. Movements in the highly specialized aquatic species were also more stereotyped with lower variability, especially at the distal-most segments as suggested by the fact that they occupy only a small part of the kinematic space (Fig. 6).

Ecological differences

A factor analysis performed on the mean kinematic variables per individual extracted four axes jointly explaining 79 percent of the overall variability in the data set (Table 3). Whereas the first axis (35.68%) was principally determined by extension of the limb, the velocity at the hip, knee, and ankle as well as the total angular change at the hip and knee, the second axis (18.42%) was determined by the changes

in mid-foot angle as well as the minimal midfoot angles (Table 3). The third axis (14.2%) was determined by the pelvic shift and the change in pelvic angle (Table 3). The fourth axis (10.85%) was determined by the relative velocity of the animal (Table 3).

A multivariate analysis of variance performed on the raw kinematic variables that showed scores greater than 0.7 on the first two axes indicated a highly significant difference in swimming kinematics in animals with different ecologies, irrespective of the fact whether *B. orientalis* was classified as aquatic or semi-aquatic (*B. orientalis* aquatic: Wilks' lambda = 0.095; $F_{20,26}$ = 2.92; P = 0.006; *B. orientalis* semi-aquatic: Wilks' lambda = 0.040; $F_{20,26}$ = 5.22; P < 0.001). For the analysis with *B. orientalis* classified as aquatic, the subsequent univariate anova's indicated that this difference was due to a significant effect on the delta knee angle, the delta hip angle, and the delta and minima of the midfoot 1 and midfoot 2 angles (Table 4). Post-hoc tests indicated that differences were significant between aquatic and terrestrial species in the delta hip angle with terrestrial species having a larger overall rotation at the hip. Moreover, differences were significant between the semi-aquatic species on the one hand and the aquatic and terrestrial species on the other hand for all midfoot angles with semi-aquatic species having larger minimal angles yet smaller overall changes in angle. The only exception was for the minimal midfoot 2 angle where aquatic and semi-aquatic species did not differ. For the analysis with *B. orientalis* classified as semi-aquatic the univariate anova's also indicated differences in the angular excursion at the hip and the midfoot (Table 4). Results of Bonferroni post-hoc tests showed identical results as the analyses with *B. orientalis* classified as aquatic.

Phylogeny

A plot of the phylogeny in the kinematic space constructed by using species means suggests that phylogeny is not driving the observed results (Fig. 6). For example, whereas the two terrestrial species *B. calamita* and *R. guttatus* are more closely related to *P. esculenta* they fall out with the terrestrial archeobatrachian *P. fuscus* (Fig. 6). Thus the structuring in the kinematic space represents ecological affinities rather than representing phylogeny. The factor analysis performed on the species means shows a similar structuring as that observed using the individual data.

Discussion

Our results showed interesting differences in swimming behavior between species with different ecologies. Semi-aquatic species stood out by the lack of changes in the midfoot angle during the extension phase which is maintained rather stable. This is in contrast to specialized aquatic species such

as *X. laevis* and terrestrial species such as *P. fuscus* and *R. guttatus* where the midfoot actively contributes to generating propulsion. These results confirm previously published data on frog swimming (Richards, 2010) that demonstrated that the highly specialized aquatic *X. laevis* obtained nearly 100% of the total thrust during swimming through foot rotation involving tarso-metatrasal extension. Other species such as the semi-aquatic *R. pipiens* or the terrestrial *B. americanus* had strong translational components to the kick. Interestingly, our analysis on species means suggest that terrestrial species had greater angular changes at the hip compared to aquatic and semi-aquatic species.

However, our results also show differences compared to previous studies. Notably, whereas Richards (2010) found that foot rotation was greater in *X. laevis* compared to *B. americanus* our results show that at least one of the bufonids (*R. guttatus*) shows greater foot rotation than *X. laevis*. The other species of bufonid included in our study (*B. calamita*), however, clustered with aquatic or semi-aquatic species depending on the classification of *B. orientalis* as aquatic or semi-aquatic (Fig. 6). Moreover, *B. calamita* also showed early knee extension as has been observed for *B. americanus* in contrast to the other terrestrial species in our data set (Fig. S2). This suggests that differences in kinematic strategies may exist within groups of closely related species with similar life-styles. Further studies exploring swimming strategies in terrestrial bufonids would be especially insightful in this context.

In addition to confirming previous results (Richards, 2010), our results show significant differences between species with different ecologies. Indeed, our kinematic analysis showed that terrestrial species were significantly different from aquatic and semi-aquatic ones. Moreover, as our analysis included both primitive and derived species, this suggests that it is not a phylogenetic effect, but likely driven by the constraints of locomotion in different media. This is confirmed by the analysis on species means where a plot of the phylogeny in the kinematic space showed that structuring is largely according to ecological grouping rather than phylogeny (Fig. 7). Although differences between species and ecological groups were rather robust, the *B. calamita* included in our data set fell within the kinematic space of both highly specialized aquatic and semi-aquatic species suggesting that interesting differences in locomotor strategies may exist within ecological groups as well. Moreover, our analysis on the individual means showed that one of the *P. esculenta* used in our analysis differed strongly from the other individual by showing much slower limb extension and a much lower contribution of the mid-foot to overall propulsion. This result is hard to explain given the tight clustering around the species means of all other individuals used in the analyses. One possible explanation may be that this was a sub-adult individual. If so this may suggest that locomotor strategies vary throughout ontogeny, yet this remains to be tested.

Of the kinematic variables measured, those associated with the sliding of the pelvis did not contribute to the overall variation in kinematics of swimming. Yet, the highly specialized sliding pelvis of pipids has previously been suggested to play an important role during swimming by increasing the length of the power stroke (Palmer, 1960; Videler and Jorna, 1985). Despite the fact that two pipids were included in our data set the average values of pelvic sliding were only slightly greater than those observed in other species that do not possess a high specialized sacral joint allowing extensive sliding of the pelvis (Supplementary figure S6). Moreover, rather than lengthening the distance between the tip of the ilium and the tip of the sacrum decreased suggesting a forward sliding of the pelvis relative to the sacral joint during the extension phase of swimming. This suggests that the role of the pelvic joint needs to be re-evaluated and that its function may be related to escape behavior or even burrowing as previously suggested (Whiting, 1961; Videler and Jorna, 1985).

Although previous studies found no trade-off between jumping and swimming kinematics or performance (Peters et al., 1996; Kamel et al., 1996; Nauwelaerts et al., 2007) our results suggest subtle but important differences in the kinematics of swimming that may be the result of specializations to different life-styles. The principal differences observed are overall changes at the hip that appear to characterize terrestrial species, and differences in the kinematics of the distal limb elements, more specifically the foot that appear to characterize semi-aquatic species. Whereas aquatic and terrestrial species appear to actively recruit the foot in generating propulsion, semi-aquatic species appear to have a relatively invariant foot angle throughout the limb extension cycle. This may be due to stiffer distal elements which may diminish the potential for the foot to contribute to the generation of propulsion, yet this remains to be examined further. These results also suggest that locomotor inferences on extinct animals may benefit from an examination of these distal elements rather than the often used proximal elements such as the hip and proximal femur (e.g. Jorgensen and Reilly, 2013; Venczel and Szentesi, 2012). Unfortunately such elements are rare in the fossil record, thus hampering our understanding of the evolution of locomotion near the base of the anuran tree.

Materials and methods

Specimens

Two *Bombina orientalis*, one *Bufo calamita*, two *Rhaebo guttatus*, four *Discoglossus pictus*, three *Pelobates fuscus*, three *Pipa pipa*, two *Pelophylax esculenta*, and seven *Xenopus laevis* of undetermined sex yet phylogenetically different backgrounds (Fig. 1) were used in the recordings. Animals were

housed individually in a temperature controlled room and provided with food consisting of crickets, earthworms and waxworms twice weekly. For each individual, the snout-vent length, the length of the femur, the tibiofibula, and the tarso-metatarsus was measured on X-ray images of anesthetized frogs (MS222) by digitizing the proximal and distal ends of each limb segment (Table 1). All experiments were approved by the ethics committee at the University of Antwerp, Belgium.

Cineradiography

Animals were recorded in dorso-ventral view while swimming using a Phillips Optimus X-ray unit with a 14 inch image intensifier and coupled to a Redlake Imaging MotionPro 2000 high resolution digital video camera set at a recording frequency ranging from 250 frames s^{-1}. Swimming was recorded in an experimental tank of 120 by 25 by 50 cm with 10 cm of water restricting swimming to a single horizontal plane parallel to the image intensifier. Test temperature varied between 20 and 24 °C for all swimming trials. Swimming was elicited by tapping the animal at the base of the urostyle with a long, thin metal rod. In all cases the stimulus was provided by the same person and such that the frog was unaware of the rod before it touched the animal. For smaller species or species that showed a poor degree of ossification (*D. pictus*, *B. calamita*), small radio-opaque markers were implanted at the different limb joints of interest to facilitate the analysis of the kinematic data. Markers were implanted percutaneously using hypodermic needles under full anesthesia with MS222.

Five swimming sequences were recorded for each individual and those where the frog stayed in the plane parallel to the image intensifier were retained for analysis. This resulted in 9 sequences for two individuals of *B. orientalis*, 17 sequences for four individuals of *D. pictus*, 26 sequences for seven individuals of *X. laevis*, eight sequences for three *P. pipa*, 16 sequences for 4 *P. fuscus*, five sequences for one *B. calamita*, eight sequences for two *R. guttatus*, and nine sequences for two *P. esculenta* for a total of 98 analyzed sequences.

On each frame, 21 landmarks were digitized for the limb extension cycle using Didge (version 2.2.0.; A. Cullum) (Fig. 2) and the X- and Y-coordinates for each point were exported to a spreadsheet. Landmarks used were (numbers indicated for one side only; see Fig. 2): the tip of the snout (1), the center of the sacrum (2), the distal end of the ischium (3), the left and right iliosacral joints (4), the left and right proximal head of the femur (5), the left and right distal end of the femur (6), the left and right proximal end of the tibiofibula (7), the left and right distal end of the tibiofibula (8), the left and right proximal end of the proximal tarsals (9), the left and right distal end of the tarsal bones (10), the left and right

distal end of the longest metatarsal (11), and the left and right distal end of the terminal phalanx of the longest toe (12). Next, coordinates were re-calculated to a frame of reference moving with the frog and with the X-axis parallel to the midline of the frog and the Y-axis going through the sacrum, thus making landmark 2 the origin of our new reference frame.

Based on the X- and Y-coordinates of these landmarks the following kinematic variables were calculated: the pelvic angle, being the angle subtended by the lines interconnecting landmarks 1 and 3 and 2 and 3 respectively; the hip angle, being the angle subtended by the lines interconnecting landmarks 1 and 3 and 5 and 6 respectively; the knee angle, being the angle subtended by the lines interconnecting landmarks 5 and 6 and 7 and 8 respectively; the ankle angle, being the angle subtended by the lines interconnecting landmarks 7 and 8 and 9 and 10 respectively; the mid-foot 1 angle, being the angle subtended by the lines interconnecting landmarks 9 and 10 and 10 and 11 respectively; the mid-foot 2 angle, being the angle subtended by the lines interconnecting landmarks 10 and 11 and 11 and 12 respectively. The hip angle, knee angle, ankle angle and both mid-foot angles were calculated for both limb pairs. Additionally, the amount of pelvic sliding was calculated as the difference in the X-coordinate between markers 2 and 4. Finally, limb extension was calculated as the difference in the X-coordinate between marker 2 and a virtual tibio-tarsal joint marker calculated as the average between the X-coordinates of markers 8 and 9 respectively.

The displacements of all limb segments were plotted against time and smoothed using a zero phase shift 4th order low pass butterworth filter with user defined cut-off frequency that was set iteratively to obtain smooth acceleration profiles without losing information in the displacement and velocity profiles (Winter, 2004). Next, the limb extension cycle was interpolated over 50 time-points allowing us to compare cycles across individuals and species. After interpolation the velocity and acceleration of displacements and angular changes were calculated based on numerical differentiation of the displacement profiles. For statistical analysis, the peak snout velocity, peak snout acceleration, average velocity, the amount of pelvic sliding, the total limb extension, the peak limb extension and retraction velocity, the delta pelvic angle, the delta hip angle, the minimal hip angle, the minimal and maximal angular velocity at the hip (i.e. associated with hip extension and flexion respectively), the delta knee angle, the minimal knee angle, the minimal and maximal angular velocity at the knee, the delta ankle angle, the minimal ankle angle, the minimal and maximal angular velocity at the ankle, the delta and minimal mid-foot 1 angles, and the delta and minimal mid-foot 2 angles were extracted (Table 2). As

limb movements are not always perfectly symmetrical, the largest angular displacement and velocity of the right and left side was retained for further analysis.

Statistical analysis

Species were classified into three broad ecological groups based on literature data. We considered as aquatic species, species that spend most of their time in water outside of the breeding season. As such *X. laevis*, *P. pipa* and *B. orientalis* (Kaplan, 1992; Du Preez and Carruthers, 2009; Ouboter and Jairam, 2012) were all classified as aquatic. As terrestrial species we considered species that spend most of their time away from water outside the breeding season. These species thus cannot be found in the immediate vicinity of water outside the breeding season and include *B. calamita*, *P. fuscus* and *R. guttatus* (Arnold and Ovenden., 1978; Ouboter and Jairam, 2012). Finally, we classified as semi-aquatic, species that live near water outside of the breeding season, yet typically jump into the water as an escape response. These species included *D. pictus* and *P. esculenta* (Arnold and Ovenden., 1978). However given conflicting statements in the literature concerning *B. orientalis* we ran all our analysis with this species classified both as aquatic and as semi-aquatic.

Next, all raw kinematic variables were averaged per individual. All variables were Log_{10}-transformed and used as input for regression analysis with SVL as the independent variable. Where significant, residuals were extracted and saved as variables. Next kinematic data (residual for those variables dependent on overall size) were used as input for a factor analysis with varimax rotation. Factors with eigenvalues over 1 were extracted and factor scores were saved. Factor scores were used to explore how species were distributed in kinematic space and to select kinematic variables for subsequent analysis. We selected all variables with loadings higher than 0.7 on the first two axes as input for a multivariate analysis of variance coupled to subsequent univariate ANOVAs. Bonferroni post-hoc tests were then used to examine which groups differed from one another for each variable that showed significant effects.

As species cannot be considered as independent data points or disconnected from their evolutionary history comparative analysis have been advocated to take into account shared ancestry in explaining patterns of phenotypic or functional diversity. However, these approaches typically require a minimum number of species for these analyses to be robust. Given the time-consuming nature of kinematic analyses our data set remains restricted. Thus, rather than doing explicit comparative analyses we decided to map the phylogeny onto the functional space, allowing us to evaluate whether structuring is driven by phylogeny or not. We did so using the phylomorphospace function in R (R Development Core

Team, 2011) implemented in the 'phytools' library (Revell, 2012). We use two alternative phylogenies that differ in the placement of the basal most taxa (Pipoidea versus Bombinatoroidea) based on the phylogenies provided by Frost et al. (2006) and Zhang et al. (2013) and pruned down to include only the taxa in our analyses (Fig. 1A, B). Moreover we classified *B. orientalis* both as aquatic and as semi-aquatic. Branch lengths were computed using the Grafen method (1989) with the "compute.brlen" function of the 'Ape' library (Paradis et al., 2012) in R (R Development Core Team, 2011).

Acknowledgements

This research was supported by a BWS-BOF bilateral cooperative project between Belgium and the Czech Republic (4/EO1514), an Agence Nationale de la Recherche (ANR) MOBIGEN grant [ANR-09-PEXT-003], and a Muséum National d'Histoire Naturelle 'Action Transversale Muséum' (MNHN) ATM grant of the programme 'Biodiversité actuelle et fossile' to A.H.

References

Abourachid, A. and Green, D. M. (1999). Origins of the frog kick? Alternate-leg swimming in primitive frogs, families Leiopelmatidae and Ascaphidae. *J. Herpetol.* **33**, 657-663.

Arnold, E. N. and Ovenden, D. (1978) Collins field guide to the reptiles and amphibiens of Britain and Europe. London: Harper Collins Ltd.

Barclay, O. R. (1946). The mechanics of amphibian locomotion. *J. Exp. Biol.* **23**, 177-203.

Calow, L. J. and Alexander, R. McN. (1973). A mechanical analysis of a hind leg of a frog *Rana temporaria*. *J. Zool., Lond.* **171**, 293-321.

Clemente, C. J. and Richards, C. (2013). Muscle function and hydrodynamics limit power and speed in swimming frogs. *Nat. Comm.* **4**, 2737. doi:10.1038/ncomms3737.

du Preez, L. and Carruthers, V. (2009) A complete guide to the frogs of Southern Africa. Cape Town: Struik Nature.

Emerson, S. B. (1976). Burrowing in frogs. *J. Morphol.* **149**, 437-457.

Emerson, S. B. (1979). The ilio-sacral articulation in frogs: form and function. *Biol. J. Linn. Soc.* **11**, 153-168.

Emerson, S. B. and De Jongh, H. J. (1980). Muscle activity at the ilio-sacral articulation of frogs. *J. Morphol.* **166**, 129-144.

Essner, R. L., Suffian, D. J., Bishop, P. J. and Reilly, S. M. (2010). Landing in basal frogs: evidence of saltational patterns in the evolution of anuran locomotion. *Naturwissenschaften* **97**, 935-939.

Estes, R. and Reig, O. A. (1973). The early fossil record of frogs: a review of the evidence. In Evolutionary *biology of the anurans* (ed. J. L. Vial), pp. 11-63. Colombia: University of Missouri Press.

Frost, D. R., Grant, T., Faivovich, J., Bain, R. H., Haas, A., Haddad, C. F. B., De Sa, R. O., Channing, A., Wilkinson, M., Donnellan, S. C., Raxworthy, C. J., Campbell, J. A., Blotto, B. L., Moler, P., Drewes, R. C., Nussbaum, R. A., Lynch, J. D., Green, D. M. and Wheeler, W. C. (2006). The amphibian tree of life. *Bull. Am. Mus. Nat. Hist*. **297**, 1-370.

Gal, J. M. and Blake, R. W. (1988). Biomechanics of frog swimming: II. Mechanics of the limb-beat cycle in *Hymenochirus Boettgeri*. *J. Exp. Biol.* **138**, 413-429.

Gans, C. and Parsons, T. (1966). On the origin of the jumping mechanism in frogs. *Evolution* **20**, 92-99.

Gillis, G. B. and Biewener, A. A. (2000). Hindlimb extensor muscle function during jumping and swimming in the toad (*Bufo marinus*). *J. Exp. Biol.* **203**, 3547-3563.

Grafen, A. (1989). The phylogenetic regression. *Phil. Trans. R. Soc. Lond. B.* **326**, 119-157.

Jenkins, F. A. and Shubin, H. H. (1998). *Prosalirus bitis* and the anuran caudopelvis mechanism. *J. Vert. Paleontol.* **18**, 495-510.

Johansson, L. C. and Lauder, G. V. (2004). Hydrodynamics of surface swimming in leopard frogs (*Rana pipiens*). *J. Exp. Biol.* **207**, 3945-3958.

Jorgensen, M. E. and Reilly, S. M. (2013). Phylogenetic patterns of skeletal morphometrics and pelvic traits in relation to locomotor modes in frogs. *J. Evol. Biol.* **26**, 929-943.

Kamel, L. T., Peters, S. E. and Bashor, D. P. (1996). Hopping and swimming in the leopard frog, *Rana pipiens*: II. A comparison of muscle activities. *J. Morphol.* **230**, 17-31.

Kaplan, R. H. (1992) Greater maternal investment can decrease offspring survival in the frog *Bombina orientalis*. *Ecology* **73**, 280-288.

Lutz, G. J. and Rome, L. C. (1994). Built for jumping: the design of the frog muscular system. *Science* **263**, 370-372.

Moen, D. S., Irschick, D. J. and Wiens, J. J. (2013). Evolutionary conservatism and convergence both lead to striking similarity in ecology, morphology and performance across continents in frogs. *Proc R. Soc. Lond. B.* **280**, 20132156.

Nauwelaerts, S. and Aerts, P. (2002). Two distinct gait types in swimming frogs. *J. Zool., Lond.* **258**, 183-188.

Nauwelaerts, S. and Aerts, P. (2003). Propulsive impulse as a covarying performance measure in the comparsion of the kinematics of swimming and jumping in frogs. *J. Exp. Biol.* **206**, 4341-4351.

Nauwelaerts, S. and Aerts, P. (2006). Take-off and landing forces in jumping frogs. *J. Exp. Biol.* **209**, 66-77.

Nauwelaerts, S., Aerts, P. and D'Aout, K. (2001). Speed modulation in swimming frogs. *J. Motor Behav.* **33**, 265-272.

Nauwelaerts, S., Scholliers, J. and Aerts, P. (2004). A functional analysis of how frogs jump out of water. *Biol. J. Linn. Soc.* **88**, 413-420.

Nauwelaerts, S., Stamhuis, E. and Aerts, P. (2005a). Swimming and jumping in a semi-aquatic frog. *Anim. Biol*. **55**, 3-15.

Nauwelaerts, S., Stamhuis, E. and Aerts, P. (2005b). Propulsive force calculations in swimming frogs I. A momentum-impulse approach. *J. Exp. Biol.* **208**, 1435-1443.

Nauwelaerts, S., Ramsay, J. and Aerts, P. (2007). Morphological correlates of aquatic and terrestrial locomotion in a semi-aquatic frog, *Rana esculenta*: no evidence for a design conflict. *J. Anat.* **210**, 304-317.

Olson, J. M. and Marsh, R. L. (1998). Activation patterns and length changes in hindlimb muscles of the bullfrog *Rana catesbeiana* during jumping. *J. Exp. Biol.* **201**, 2763-2777.

Ouboter, P. E. and Jairam, R. (2012) Amphibians of Suriname. Leiden: Brill.

Palmer, M. (1960). Expanded ilio-sacral joint in the toad *Xenopus laevis*. *Nature* **187**: 757.

Paradis, E., Bolker, B., Claude, J., Cuong, H. S., Desper, R., Durand, B., Dutheil, J., Gascuel, O., Heibl, C., Lawson, D., Lefort, V., Legendre, P., Lemon, J., Noel, Y., Nylander, J., Opgen-Rhein, R., Popescu, A.-A., Schliep, K., Strimmer, K. and de Vienne, D. (2012). ape: Analyses of phylogenetics and evolution in R language. *Bioinformatics* **20**, 289-290.

Peters, S. E., Kamel, L. T. and Bashor, D. P. (1996). Hopping and swimming in the Leopard Frog, *Rana pipiens*: I. Step cycles and kinematics. *J. Morphol.* **230**, 1-16.

Prikryl, T., Aerts, P., Havelková, P., Herrel, A. and Rocek, Z. (2009). Pelvic and thigh musculature in frogs (Anura) and origin of anuran jumping locomotion. *J. Anat.* **214**, 100-139.

R Development Core Team (2011). R: A language and environment for statistical computing. R Foundation for Statistical Computing. Vienna: R Foundation for Statistical Computing. Available at: http://www.R-project.org.

Reilly, S. M. and Jorgensen, M. E. (2011). The evolution of jumping in frogs: morphological evidence for the basal anuran locomotor condition and the radiation of locomotor systems in crown group anurans. *J. Morphol.* **272**, 149-168.

Revell, L. J. (2012). phytools: An R package for phylogenetic comparative biology (and other things). *Methods Ecol. Evol.* **3**, 217-223.

Richards, C. T. (2008). The kinematic determinants of anuran swimming performance: an inverse and forward dynamics approach. *J. Exp. Biol.* **211**, 3181-3194.

Richards, C. T. (2010). Kinematics and hydrodynamics analysis of swimming anurans reveals striking interspecific differences in the mechanism for producing thrust. *J. Exp. Biol.* **213**, 621-634.

Richards, C. T. and Biewener, A. A. (2007). Modulation of in vivo muscle power output during swimming in the African clawed frog (*Xenopus laevis*). *J. Exp. Biol.* **210**, 3147-3159.

Shubin, N. H. and Jenkins, F. A. (1995). An early jurassic jumping frog. *Nature* **377**, 49-52.

Sigurdsen, T., Green, D. M. and Bishop, P. J. (2012). Did *Triadobatrachus* jump? Morphology and evolution of the anuran forelimb in relation to locomotion in early salientians. *Fieldiana* **5**, 77-89.

Stamhuis, E. and Nauwelaerts, S. (2005). Propulsive force calculations in swimming frogs II. Application of a vortex ring model to DPIV data. *J. Exp. Biol.* **208**, 1445-1451.

Venczel, M. and Szentesi, Z. (2012). Locomotory techniques in Upper Cretaceous frogs (Iharkut, Hungary). *Hantkeniana* **7**, 19-25.

Videler, J. J. and Jorna, J. T. (1985). Functions of the sliding pelvis in *Xenopus laevis*. *Copeia* **1985**, 251-254.

Whiting, H. P. (1961). Pelvic girdle in amphibian locomotion. Symp. *Soc. Exp. Biol.* **5**, 43-58.

Winter, D. A. (2004) *Biomechanics and Motor Control of Human Movement*. New York, NY: John Wiley and Sons.

Zhang, P., Liang, D., Mao, R. L., Hillis, D. M., Wake, D. B. and Cannatella, D. C. (2013) Efficient sequencing of anuran mtDNAs and a mitogenomic exploration of the phylogeny and evolution of frogs. Mol. Biol. Evol. doi:10.1093/molbev/mst091.

Zug, G. R. (1978). Anuran locomotion-structure and function, 2, jumping performance of semiaquatic, terrestrial and arboreal frogs. *Smithson Contrib. Zool.* **276**, 1-30.

Figure legends

Figure 1: A) Phylogenetic tree based on Frost et al., 2006 showing the relationships between the species included in this study. Indicated are also the ecologies of each species. B) Phylogenetic tree based on Zhang et al. (2013).

Figure 2: X-ray image of a *Xenopus* frog during swimming. Indicated are the points used for digitization and the kinematic variables calculated based on the X-Y coordinates of these landmarks. See methods for a description of the landmarks and angles.

Figure 3: Mean kinematic profiles for a specialized aquatic species, *Xenopus laevis*. Indicated from top to bottom are the changes in limb extension, hip angle, knee angle, ankle angle, and mid-foot 1 and mid-foot 2 angles over time. Time is standardized relative to the duration of the limb extension cycle, and the dashed lines represent one standard deviation from the mean.

Figure 4: Mean kinematic profiles for a semi-aquatic species, *Discoglossus pictus*. Indicated from top to bottom are the changes in limb extension, hip angle, knee angle, ankle angle, and mid-foot 1 and mid-foot 2 angles over time. Time is standardized relative to the duration of the limb extension cycle, and the dashed lines represent one standard deviation from the mean.

Figure 5: Mean kinematic profiles for a terrestrial species, *Pelobates fuscus*. Indicated from top to bottom are the changes in limb extension, hip angle, knee angle, ankle angle, and mid-foot 1 and mid-foot 2 angles over time. Time is standardized relative to the duration of the limb extension cycle, and the dashed lines represent one standard deviation from the mean.

Figure 6: Results of a principal component analysis performed on the raw kinematic means for each individual. A) plot of the first tow axes with *B. orientalis* classified as aquatic; B) plot of the first two axes with *B. orientalis* classified as semi-aquatic. Colors indicate the different ecologies with white symbols indicating aquatic species, black symbols indicating terrestrial species and grey symbols indicating semi-aquatic species. Symbols represent species as follows: squares, *D. pictus*; cross, *P. esculenta*; star, *B calamita*; hexagon, *R. guttatus*; diamond, *P. fuscus*; triangle up, *X. laevis*; triangle down, *P. pipa*; circle. *B. orientalis*.

Figure 7: Results of a principal component analysis performed on species means of the kinematic variables. The phylogeny is plotted in the kinematic space. Colors indicate the different ecologies with white symbols indicating aquatic species, black symbols indicating terrestrial species and grey symbols indicating semi-aquatic species. Note how species with similar ecologies are not closely related and how the structuring in kinematic space is not driven by phylogeny but rather by ecology. A) phylogeny based on Frost et al (2006) *B. orientalis* classified as aquatic; B) phylogeny based on Zhang et al. (2013) with *B. orientalis* classified as aquatic; C) phylogeny based on Frost et al (2006) *B. orientalis* classified as semi-aquatic; D) phylogeny based on Zhang et al. (2013) with *B. orientalis* classified as semi-aquatic;

Figure S1: Mean kinematic profiles for an aquatic species, *Bombina orientalis*. Indicated from top to bottom are the changes in limb extension, hip angle, knee angle, ankle angle, and mid-foot 1 and mid-foot 2 angles over time. Time is standardized relative to the duration of the limb extension cycle, and the dashed lines represent one standard deviation from the mean.

Figure S2: Mean kinematic profiles for a terrestrial species, *Bufo calamita*. Indicated from top to bottom are the changes in limb extension, hip angle, knee angle, ankle angle, and mid-foot 1 and mid-foot 2 angles over time. Time is standardized relative to the duration of the limb extension cycle, and the dashed lines represent one standard deviation from the mean.

Figure S3: Mean kinematic profiles for a terrestrial species, *Rhaebo guttatus*. Indicated from top to bottom are the changes in limb extension, hip angle, knee angle, ankle angle, and mid-foot 1 and mid-

443 foot 2 angles over time. Time is standardized relative to the duration of the limb extension cycle, and
444 the dashed lines represent one standard deviation from the mean.

445 **Figure S4**: Mean kinematic profiles for an aquatic species, *Pipa pipa*. Indicated from top to bottom are
446 the changes in limb extension, hip angle, knee angle, ankle angle, and mid-foot 1 and mid-foot 2 angles
447 over time. Time is standardized relative to the duration of the limb extension cycle, and the dashed lines
448 represent one standard deviation from the mean.

449 **Figure S5**: Mean kinematic profiles for a semi-aquatic species, *Pelophylax esculenta*. Indicated from top
450 to bottom are the changes in limb extension, hip angle, knee angle, ankle angle, and mid-foot 1 and mid-
451 foot 2 angles over time. Time is standardized relative to the duration of the limb extension cycle, and
452 the dashed lines represent one standard deviation from the mean.

453 **Figure S6**: Mean kinematic profiles describing the pelvic sliding in the different species. Time is
454 standardized relative to the duration of the limb extension cycle, and the dashed lines represent one
455 standard deviation from the mean.

Table 1: morphometric data for the specimens used for the kinematic analyses.

species	# individuals	SVL	femur	tibiofibula	tarsus
Bombina orientalis	2	52 ± 1.4	17.8 ± 1.2	18.2 ± 0.7	12.4 ± 0.3
Discoglossus pictus	4	55.8 ± 5.4	20.5 ± 2.1	20.4 ± 2.5	10.7 ± 1.5
Xenopus laevis	7	134.9 ± 19.2	42.5 ± 3.4	42.9 ± 4.0	24.7 ± 1.9
Pipa pipa	3	129.3 ± 6.0	44.4 ± 2.1	39.4 ± 2.3	21.8 ± 1.0
Pelobates fuscus	4	52.5 ± 2.5	19.2 ± 1.7	15.6 ± 1.3	8.6 ± 1.0
Bufo calamita	1	52	14.4	14.4	7.8
Rhaebo guttatus	2	129.5 ± 2.1	43.6 ± 1.8	39.5 ± 0.8	21.7 ± 2.8
Pelophylax esculenta	2	69.5 ± 21.9	30.7 ± 6.9	30.2 ± 6.7	15.1 ± 2.3

All measurements are lengths in mm. SVL, snout-vent length.

Table 2: summary swimming kinematics for the species used.

		B. orientalis	*D. pictus*	*X. laevis*	*P. pipa*	*P. fuscus*	*B. calamita*	*R. guttatus*	*P. esculenta*
snout speed	Max (m/s)	0.4 ± 0.2	0.6 ± 0.2	0.5 ± 0.2	0.5 ± 0.2	0.4 ± 0.3	0.3 ± 0.07	0.5 ± 0.09	0.5 ± 0.2
snout acc.	Min (m/s²)	-5.8 ± 6.5	-14.1 ± 15.6	-13.8 ± 12.4	-17.8 ± 13.7	-5.2 ± 5.6	-1.9 ± 0.5	-16.3± 5.1	-5.3 ± 3.5
average vel.	(m/s)	0.03 ± 0.01	0.04 ± 0.01	0.08 ± 0.03	0.08 ± 0.02	0.03 ± 0.01	0.03 ± 0.001	0.08 ± 0.02	0.05 ± 0.01
pelvic shift	Δ (mm)	1.3 ± 0.4	2.0 ± 1.7	4.1 ± 1.9	4.2 ± 2.3	2.0 ± 0.7	2.6 ± 0.9	3.7 ± 1.7	1.2 ± 0.3
limb extension	Δ (mm)	18.2 ± 5.7	33.3 ± 8.5	42.3 ± 17.6	48.8 ± 12.5	29.3 ± 8.1	20.8 ± 2.4	60.4 ± 9.0	38.8 ± 7.0
	Max vel. (mm/s)	277.1 ± 134.8	1763.1 ± 2961.0	521.4 ± 913.3	429.5 ± 201.6	2720.3 ± 8787.2	285.9 ± 101.9	750.4 ± 93.2	542.9 ± 236.6
pelvic angle	Δ (°)	4.5 ± 1.8	7.2 ± 2.4	6.2 ± 3.6	5.8 ± 2.3	8.4 ± 3.9	14.0 ± 10.0	3.2 ± 0.8	5.4 ± 3.2
hip angle	hip ^	51.6 ± 10.0	62.8 ± 15.5	50.7 ± 24.5	46.1 ± 17.6	76.9 ± 27.0	70.8 ± 4.6	70.9 ± 14.2	65.4 ± 25.6
	Min (°)	94.4 ± 11.9	90.3 ± 14.9	91.6 ± 20.2	79.7 ± 17.3	72.9 ± 16.9	55.6 ± 6.0	67.3 ± 11.7	83.8 ± 19.0
	Max vel. (°/s)	813.0 ± 333.1	1292.5 ± 453.9	428.3 ± 279.4	392.0 ± 173.4	1350.5 ± 491.6	911.8 ± 262.9	859.6 ± 51.5	1111.2 ± 747.6
knee angle	Δ (°)	93.8 ± 41.1	119.6 ± 29.6	86.8 ± 36.5	67.4 ± 22.6	112.4 ± 32.4	97.2 ± 8.3	120.8 ± 19.6	117.6 ± 25.4
	Min (°)	34.7 ± 11.5	19.7 ± 9.3	26.0 ± 16.7	26.2 ± 9.6	5.9 ± 4.2	14.8 ± 9.4	13.9 ± 5.4	20.4 ± 14.2
	Max vel. (°/s)	1455.0 ± 887.9	2587.6 ± 883.0	785.4 ± 445.0	562.8 ± 218.6	2076.0 ± 864.7	1198.4 ± 409.8	1607.2 ± 247.6	1931.1 ± 1125.0
ankle angle	Δ (°)	111.7 ± 32.6	130.7 ± 23.7	92.4 ± 26.9	51.9 ± 22.5	77.9 ± 36.3	79.8 ± 11.2	114.1 ± 34.1	112.0 ± 15.9
	Min (°)	38.9 ± 4.7	29.9 ± 10.2	50.1 ± 7.4	69.9 ± 6.5	83.2 ± 12.4	69.4 ± 11.03	21.6 ± 11.6	46.9 ± 7.1
	Max vel. (°/s)	1852.4 ± 831.7	3207.6 ± 964.9	946.8 ± 554.4	494.2 ± 201.9	1348.0 ± 609.3	1083.5 ± 384.8	1733.8 ± 322.6	1874.3 ± 924.9
midfoot 1	Δ (°)	41.4 ± 7.0	15.8 ± 5.6	71.7 ± 14.0	42.2 ± 19.5	85.0 ± 28.4	45.7 ± 11.0	78.3 ± 38.6	47.0 ± 14.4
	Min (°)	134.4 ± 6.6	160.1 ± 5.3	88.2 ± 8.6	86.3 ± 3.3	83.7 ± 14.5	121.0 ± 9.2	104.5 ± 5.6	125.2 ± 16.7
midfoot 2	Δ (°)	41.4 ± 13.6	25.3 ± 14.5	65.1 ± 21.7	54.2 ± 21.1	69.0 ± 34.4	38.4 ± 14.5	125.5 ± 24.0	51.7 ± 37.5
	Min (°)	128.6 ± 12.1	148.9 ± 14.7	104.0 ± 20.2	106.6 ± 21.0	109.2 ± 23.9	130.0 ± 13.8	58.2 ± 11.9	123.0 ± 36.5

Acc, acceleration; Δ, delta; Min, minimum; max, maximum; vel, velocity

Table 3: results of a factor analysis performed on the kinematic data.

	Factor 1	Factor 2	Factor 3	Factor 4
% variance explained	35.68	18.42	14.20	10.85
Res. min. snout acceleration	0.610	0.292	0.004	0.368
Res. average snout velocity	0.021	-0.080	0.053	**0.926**
Res. pelvic shift	0.194	-0.099	**0.706**	0.214
Res. Δ limb extension	0.600	-0.153	0.101	0.601
Res. max. hip angular velocity	**0.923**	-0.039	0.057	-0.164
Res. max. knee angular velocity	**0.959**	-0.022	-0.088	0.076
Res. max. ankle angular velocity	**0.838**	0.201	-0.371	0.146
Max. snout velocity	0.666	0.059	-0.075	0.453
Max. limb extension velocity	**0.705**	0.097	0.315	0.153
Δ pelvic angle	0.371	0.305	**0.735**	-0.104
Δ hip angle	**0.866**	-0.056	0.266	-0.204
Δ knee angle	**0.893**	0.003	0.013	0.220
Min. knee angle	-0.606	0.286	-0.304	0.403
Δ ankle angle	0.620	0.292	-0.388	0.215
Min. ankle angle	-0.328	-0.147	0.813	-0.058
Min. midfoot 1 angle	0.176	**0.774**	-0.487	0.042
Min. midfoot 2 angle	-0.086	**0.866**	0.351	-0.142
Δ midfoot 1 angle	-0.090	**-0.875**	0.232	-0.159
Δ midfoot 2 angle	0.019	**-0.959**	-0.054	0.140

Bolded loadings represent loadings greater than 0.7 and indicate variables contributing strongly to a factor.

Table 4: results of the uni-variate anova's performed on the raw kinematic data.

Variable	$F_{2,22}$	*P*
B. orientalis = aquatic		
Δ hip angle	5.13	0.015
Δ knee angle	4.61	0.021
min. midfoot 1 angle	14.90	< 0.001
min. midfoot 2 angle	3.87	0.036
Δ midfoot 1 angle	16.16	< 0.001
Δ midfoot 2 angle	8.12	< 0.001
B. orientalis = semi-aquatic		
Δ hip angle	4.81	0.018
Δ knee angle	3.44	0.05
min. midfoot 1 angle	35.27	< 0.001
min. midfoot 2 angle	4.64	0.021
Δ midfoot 1 angle	13.71	< 0.001
Δ midfoot 2 angle	8.66	0.002

Figure 01

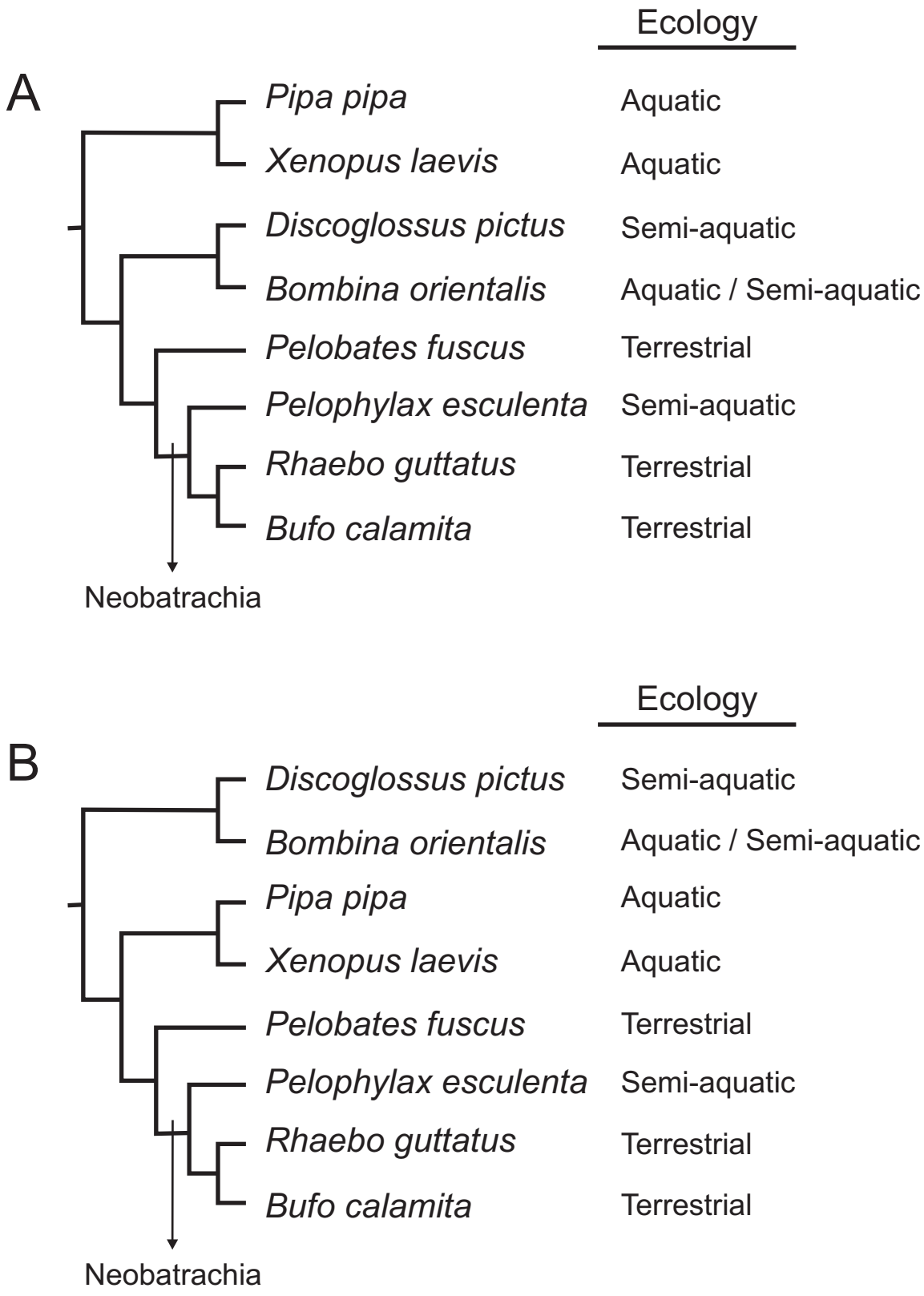

Figure 02

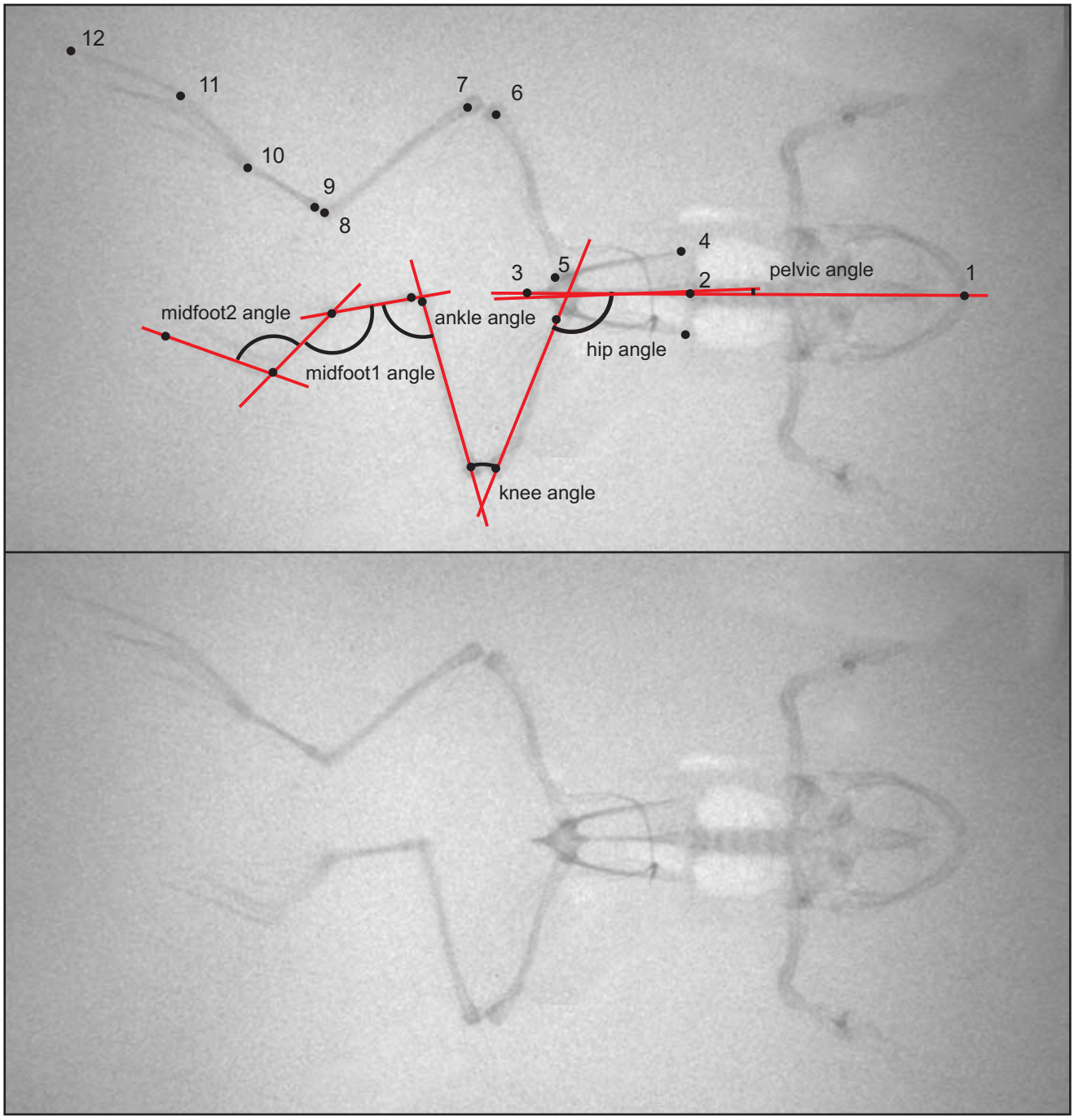

Figure 03

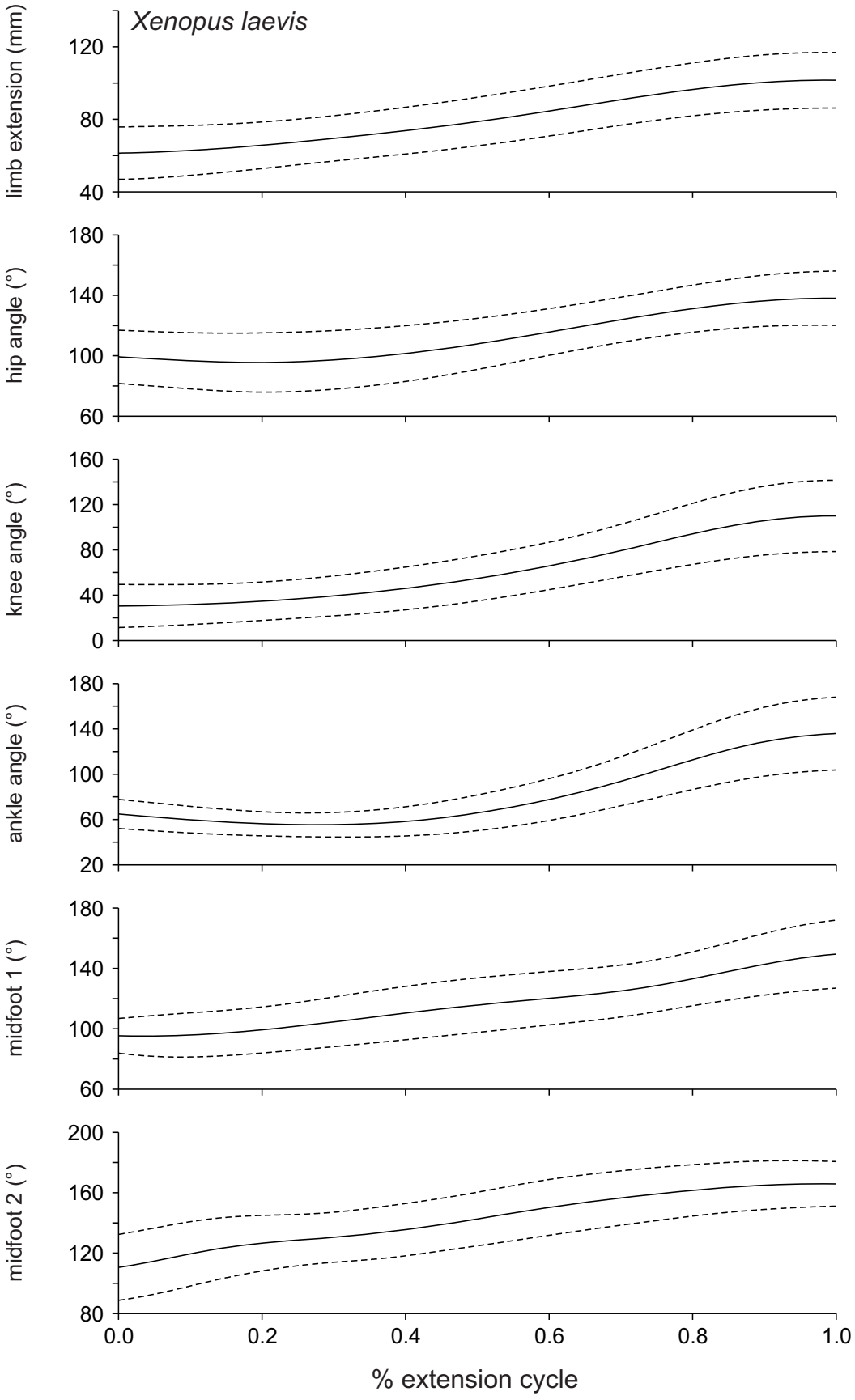

Figure 04

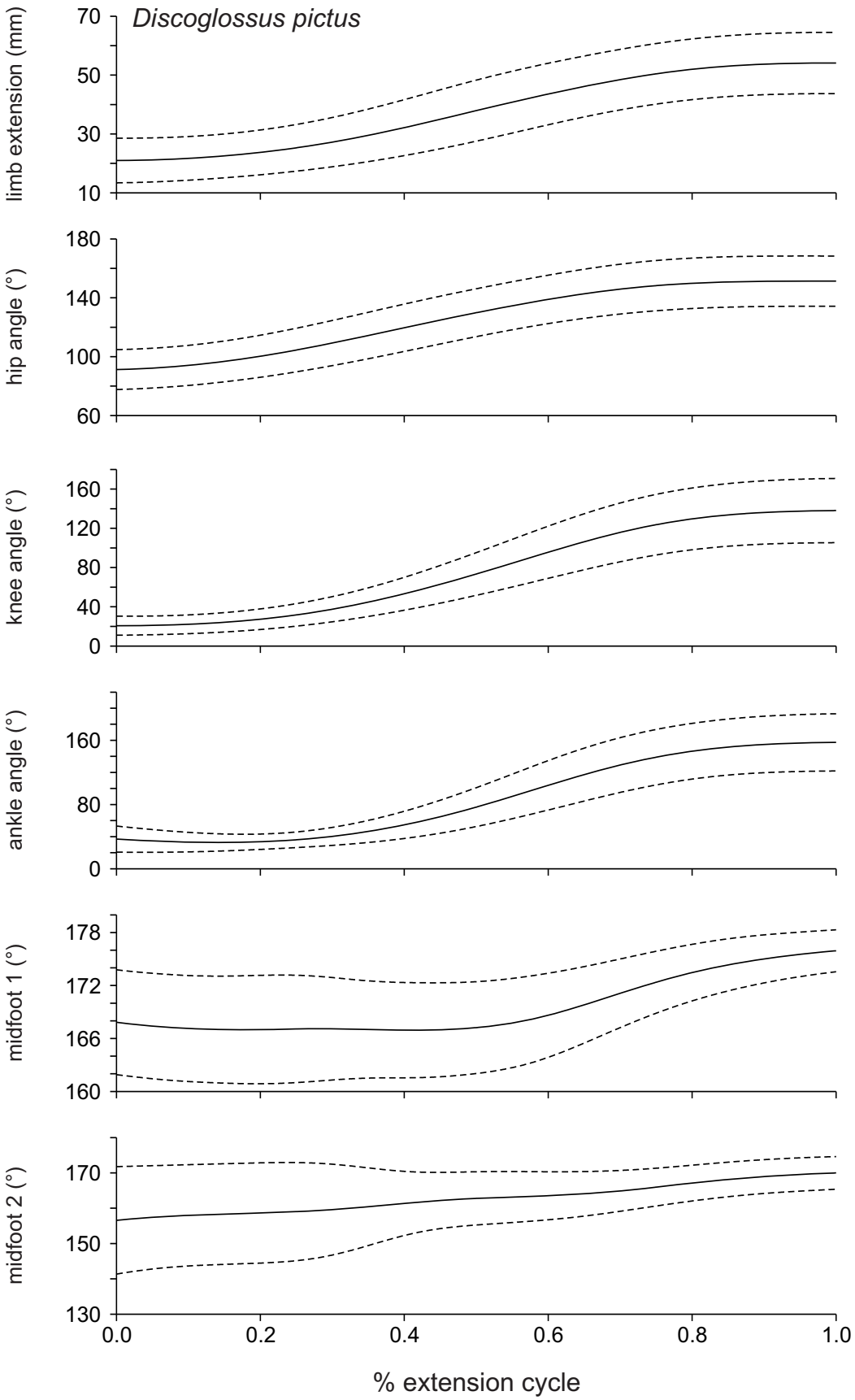

Figure 05

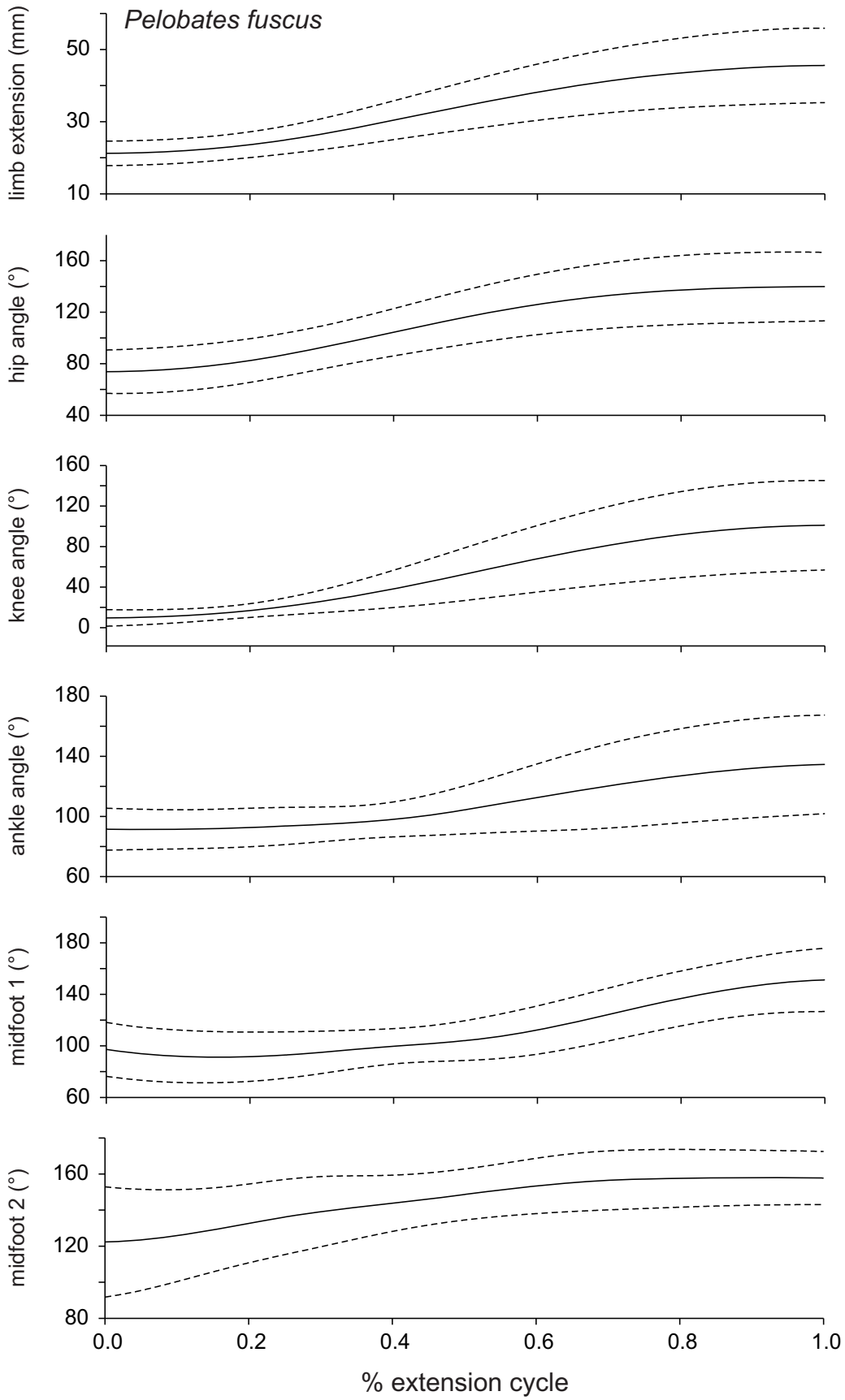

Figure 06

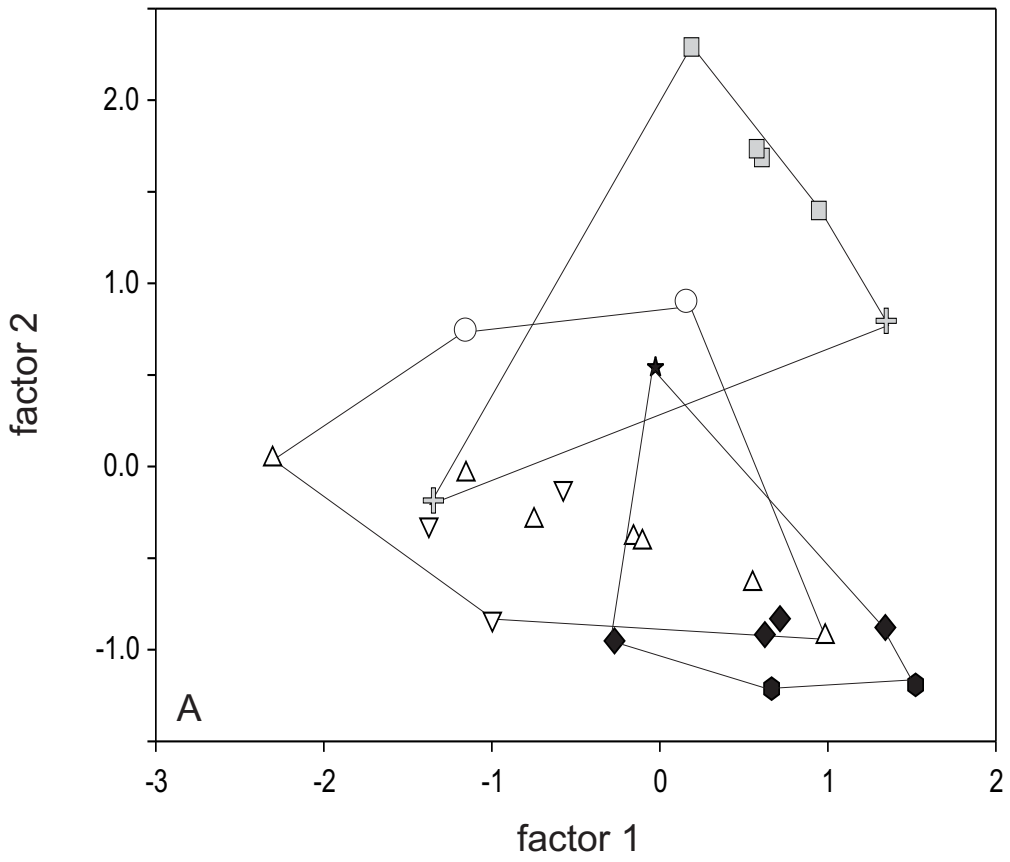

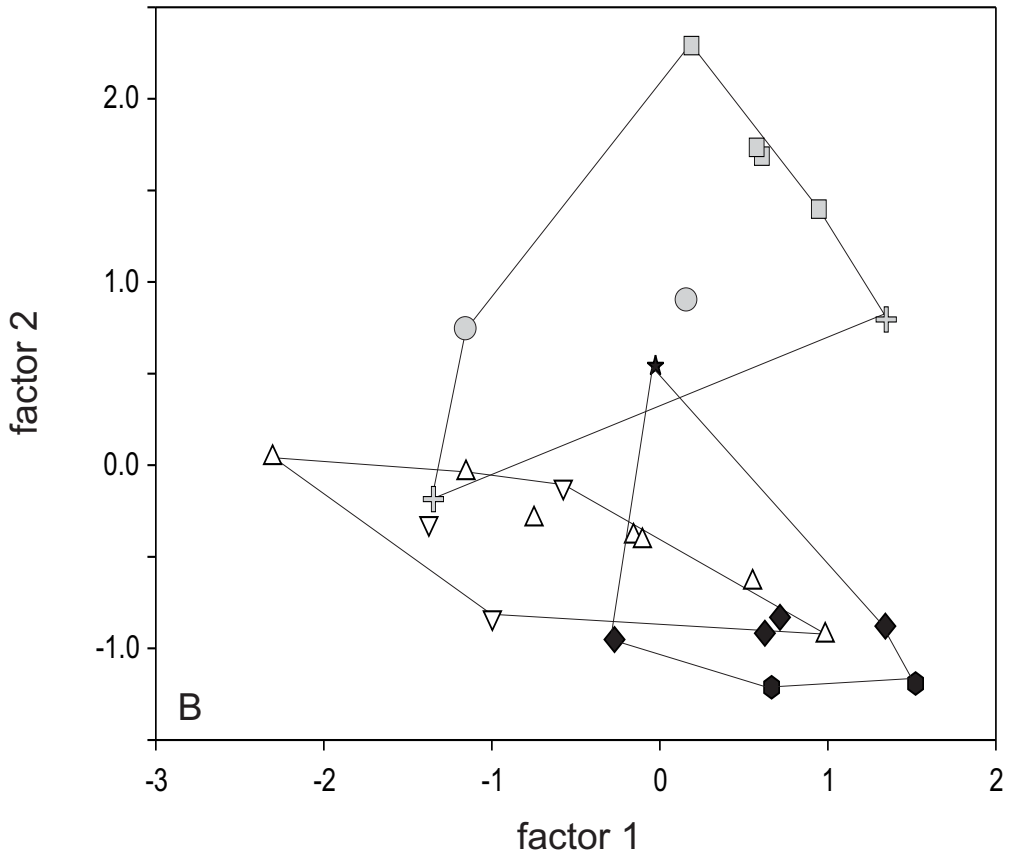

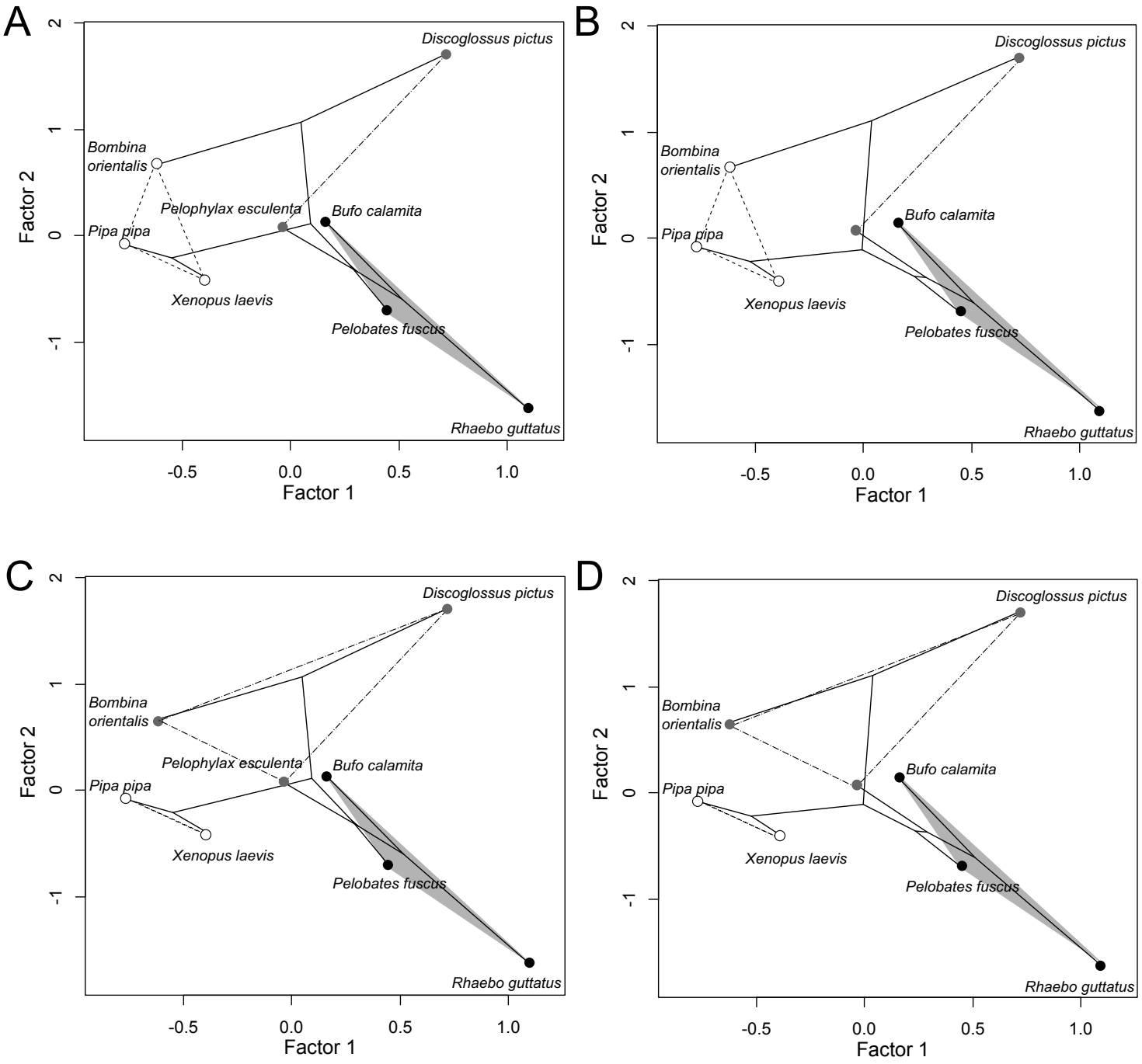
A
B
C
D
Discoglossus pictus
Bombina orientalis
Pelophylax esculenta
Bufo calamita
Pipa pipa
Xenopus laevis
Pelobates fuscus
Rhaebo guttatus
Factor 1
Factor 2
-0.5
0.0
0.5
1.0
-1
0
1
2